WiFEL: THE WISCONSIN FREE ELECTRON LASER*

R. A. Bosch#, J. J. Bisognano, M. Bissen, M. A. Green, H. Höchst,
K. D. Jacobs, K. J. Kleman, R. A. Legg, R. Reininger and R. Wehlitz,
Synchrotron Radiation Center, University of Wisconsin-Madison, Stoughton, WI 53589, U.S.A.
W. S. Graves, F. X. Kärtner and D. E. Moncton,
Massachusetts Institute of Technology, Cambridge, MA 02139, U.S.A.

Abstract

The University of Wisconsin-Madison's Synchrotron Radiation Center and the Massachusetts Institute of Technology (MIT) are developing a seeded VUV/soft x-ray free electron laser (FEL) serving multiple simultaneous users. The design uses an L-band CW superconducting 2.2 GeV linac to deliver 200 pC bunches to several FELs that cover the 5–900 eV photon range at repetition rates from kHz to MHz. The FEL output will be fully coherent longitudinally and transversely, with tunable pulse energy and variable polarization. To avoid the need for fresh electron bunches, bunch seeding at higher photon energies will be performed with high harmonic generation (HHG) laser pulses. This facility is expected to enable new science through ultrahigh resolution in the time and frequency domains, as well as coherent imaging and nanofabrication.

INTRODUCTION

The Wisconsin FEL (WiFEL) facility, whose layout is shown in Fig. 1, uses a superconducting injector and linear accelerator to provide high-quality bunches at a rate of 5 MHz with average current of one mA [1–3]. The bunches are distributed to an initial complement of six FELs using radiofrequency (rf) separation [3]. The FELs provide tunable photon energy and polarization in the first harmonic over the range of 5–900 eV, with timing and synchronization at the 10 fs level. Fully coherent photon beams are achieved by laser seeding that utilizes HHG from 4–30 eV and a harmonic cascade scheme.

FEL PERFORMANCE

Based on discussions with the scientific community and cost constraints, WiFEL is envisioned to initially have six FEL beamlines. In the future, the number of beamlines may be increased. Each beamline has at least a factor-of-three range in photon energy, as shown in Table 1. Since the beamlines operate simultaneously, the tuning strategy relies upon changing the undulator gap rather than changing the electron beam energy.

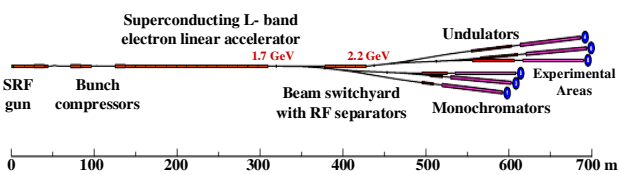

Figure 1: Layout of the WiFEL facility.

The electron beam properties include energy of 1.7 GeV for beamlines 1–3 and 2.2 GeV for beamlines 4–6, 1 kA peak current, 200 keV energy spread, 1 μm-rad normalized transverse emittance, 200 pC bunch charge, with bunch repetition rates up to 1 MHz for each beamline. To produce fully coherent photon pulses, each FEL is seeded. Seed lasers, whose properties are described in Ref. [2], use HHG covering 4–30 eV with a maximum peak power of 10 MW.

Seeding is accomplished by copropagating the seed laser and electron beam through a modulator (an undulator tuned to be resonant with the seed), and then sending the bunch through a magnetic chicane with a small R_{56} value of 1–200 μm. After the chicane converts the imprinted energy modulation to a longitudinal density modulation at the seed wavelength, the bunch enters the final radiator, which is an undulator tuned to the desired output photon energy. For energies up to 30 eV, the fundamental wavelength of the modulation is amplified, while higher energies amplify a harmonic of the nonlinearly bunched beam. To reach the highest energies, additional modulator/chicane sections provide harmonic multiplication. Figure 2 shows an example for FEL beamline 6 operating at 900 eV.

Each modulator in a cascade is relatively short (≤1 m) with little exponential gain. Since the modulation depth in each stage is modest, the bunch's energy spread remains reasonable through the cascade, allowing the use of single, short, low-charge bunches. The fresh-bunch technique requiring long, high charge (~1 nC) bunches is not needed. The low bunch charge reduces the required power and efficiency of the injector drive laser and photocathode, allows reduced linac rf power or higher bunch repetition rates, and reduces higher order mode heating and linac wakes. For WiFEL, the use of low-charge bunches allows a 5 MHz bunch repetition rate.

Modulators and early sections of the final radiators are planar undulators. To provide full polarization control of the output photons, APPLE II undulators are used for the last few gain lengths of the final radiators. If the final radiator is operated in a planar configuration, higher odd harmonics of the fundamental output energy will be produced. These may contain useful power, extending the reach of WiFEL up to 2700 eV in the third harmonic.

Calculations of FEL performance have been done with the time dependent codes Ginger [4] and Genesis [5]. Details are presented in Table 1 for each beamline

*This work is supported by the University of Wisconsin-Madison and MIT, and by NSF grant DMR-0537588.
bosch@src.wisc.edu

Table 1: FEL beamline energy ranges, and output properties for each beamline tuned to highest photon energy

FEL beamline	BL1	BL2	BL3	BL4	BL5	BL6
Photon energy range (eV)	4.4–40	20–180	180–550	80–550	250–750	300–900
Wavelength (nm)	31.0	6.9	2.3	2.3	1.65	1.37
Peak power (GW)	3.0	3.0	1.4	2.3	1.6	1.2
Photons per pulse	1.3×10^{13}	3.8×10^{12}	4.9×10^{11}	7.2×10^{11}	2.8×10^{11}	1.5×10^{11}
Pulse energy (μJ)	80	110	43	63	34	22
Rms pulse length (fs)	9.3	11.0	9.0	8.3	7.3	6.4
Rms bandwidth (meV)	43	60	102	93	110	128
Coherence length (fs)	41	35	22	24	19	16
Peak brilliance (photons/s/0.1%/ mm^2 mrad^2)	3.8×10^{29}	5.6×10^{30}	3.2×10^{31}	5.4×10^{31}	5.3×10^{31}	4.9×10^{31}
Average brilliance(p/s/0.1%/ mm^{2}mr^2 at 1MHz)	3.5×10^{21}	6.2×10^{22}	2.9×10^{23}	4.4×10^{23}	3.9×10^{23}	3.1×10^{23}
Peak flux (photons/s)	5.0×10^{26}	1.1×10^{26}	2.1×10^{25}	3.0×10^{25}	1.3×10^{25}	8.1×10^{24}
Average flux (photons/s at 1 MHz)	1.3×10^{19}	3.8×10^{18}	4.9×10^{17}	7.2×10^{17}	2.8×10^{17}	1.5×10^{17}
Rms source size (μm)	85	42	42	44	36	33
Rms diffraction angle (μrad)	44	20	4.7	4.5	3.9	3.6
M^2	1.50	1.56	1.07	1.10	1.07	1.06
Waist location (m before undulator end)	1.4	6.7	8.2	6.4	6.8	7.0
Rayleigh length (m)	2.0	2.1	8.8	9.6	9.2	9.1

operating at its highest energy. Monochromators with up to 10^5 resolving power are provided for narrow bandwidth experiments.

ELECTRON GUN

The proposed superconducting rf gun is a 200 MHz quarter wave resonator design [2]. The University of Wisconsin-Madison and Niowave Inc. have produced detailed engineering drawings, as shown in Fig. 3. This design work and our collaboration with the Naval Postgraduate School in the construction and testing of their superconducting rf gun will enable us to produce a cost-effective prototype device.

The gun produces self inflating bunches with uniform density. These are created when an ultra-short laser pulse is directed onto the photocathode to produce a charge pancake which then "blows out" into a uniform ellipsoid under its own self space charge fields.

The low rf frequency has several advantages. The device can operate at 4.2 K since the BCS losses go as the frequency squared. The accelerating gap is small compared to the rf wavelength, making the device nearly DC in performance. This minimizes the effect of phase slip as the bunch traverses the gap, producing a bunch with a linear momentum versus position distribution.

The cathode holder is warmer than the cavity, allowing the use of a Cs_2Te cathode with quantum efficiency orders of magnitude higher than a metal cathode. This greatly reduces the power and photon energy of the drive laser, decreasing its cost and complexity. A coaxial half-wave cavity filter, shown in Fig. 4, provides an rf short circuit between the cathode and the cavity while providing a thermal break.

For emittance compensation, a superconducting ferromagnetic solenoid located near the cathode uses niobium wire cooled via copper straps to the He cryostat. The rf coupler uses a hard coupling from the input feedthrough to the center conductor to provide sufficient coupling. The flange at the shorted end of the coupler is a water-cooled heat sink for the coupler's inner conductor, limiting the re-radiation of heat into the cavity.

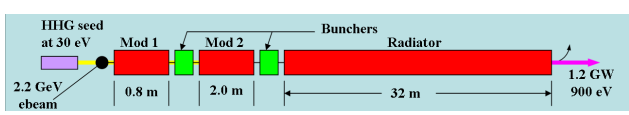

Figure 2: Undulator line for beamline 6 operating at 900 eV. The HHG seed laser at 30 eV is upconverted by a factor of 30 in a three stage harmonic cascade, to produce over 1 GW of output power in a 20 fs FWHM pulse.

COMPRESSION

The WiFEL driver uses superconducting linacs and magnetic compression to transform a 4 MeV bunch with peak current of 50 A into a 1.7 GeV bunch with peak current of 1 kA [3]. The initial bunch has normalized

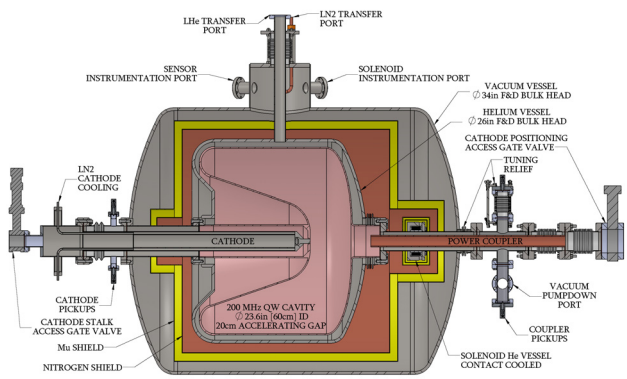

Figure 3: Quarter wave resonator gun, cryostat, cathode holder and rf power coupler.

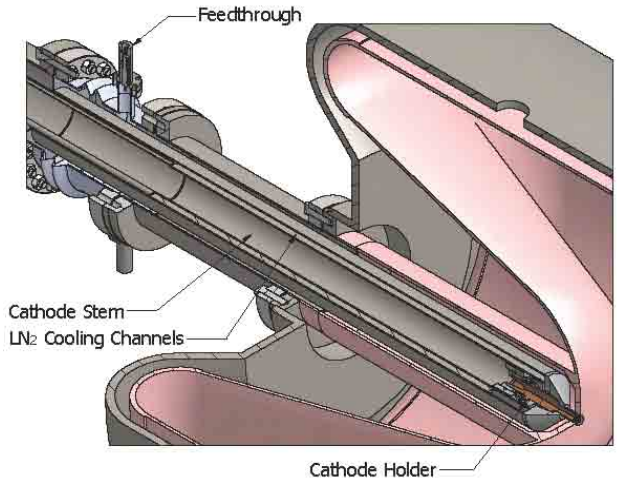

Figure 4: Coaxial cavity filter and cathode holder.

transverse emittance of 1 μm-rad, charge of 200 pC, 3 keV rms Gaussian energy spread, and a parabolic longitudinal distribution with rms length of 0.4 mm. The bunch is then distributed to an FEL and collimated by a three-level beam spreader.

In our preliminary two-stage compressor of Fig. 5(a), the first chicane compresses by a factor of 8 at energy of 215 MeV while the second chicane compresses by 2.5 at 485 MeV [3, 6]. The bunch is then distributed by a beam spreader whose R_{56} value is 950 μm.

A reduction in microbunching was obtained with a single-stage compressor at energy of 400 MeV, shown in Fig. 5(b), followed by a beam spreader with a low R_{56} value of 38.5 μm. Figure 6 shows the dramatic reduction in amplified noise in ELEGANT [7] simulations that model the amplified shot noise of a 200 pC bunch [8].

LOW-R_{56} BEAM SPREADER

At an energy of 1.7 GeV, a three-level beam spreader sends each compressed bunch to a 1.7 GeV FEL or a 2.2 GeV FEL. Rf cavities are chosen for beam distribution because the high bunch repetition rate precludes the use of pulsed magnets. A pair of normal-conducting TEM-mode cavities provides a kick of ±1.6 mrad [9]. The spreader splits the incoming bunch train into eight trains with one-eighth of the input repetition rate. The frequency of the m-th level separator

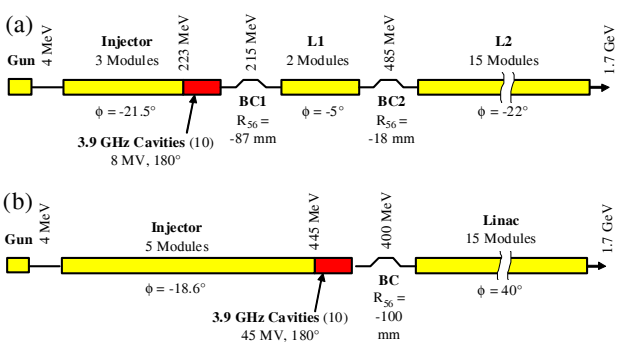

Figure 5: Schematic diagrams for two bunch compressors. (a) Two-stage compressor. (b) Single-stage compressor.

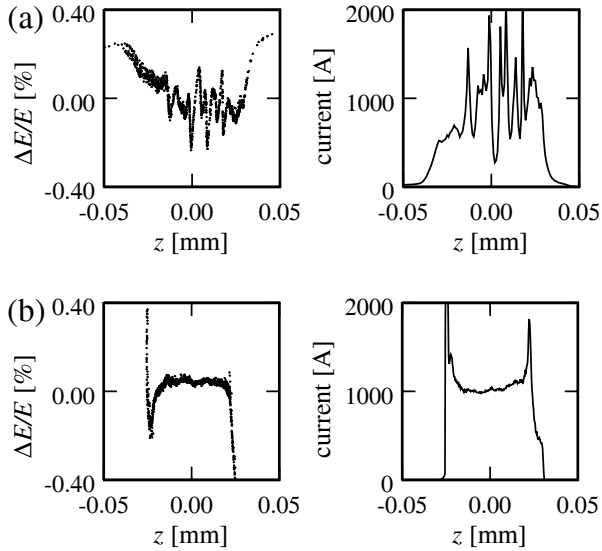

Figure 6: Longitudinal phase space and current profile at the entrance of a 1.7 GeV FEL, for a bunch with initial 3 keV rms Gaussian energy spread. The tail is on the right. We model the shot noise of 1.25×10^9 electrons by tracking 8×10^6 particles whose longitudinal space-charge wake upstream of the first chicane is reduced by $(1.25\times10^9/8\times10^6)^{1/2}$. (a) Two-stage compressor followed by a beam spreader with R_{56} = 950 μm. (b) Single-stage compressor followed by a spreader with R_{56} = 38.5 μm.

cavities is $f_b\,(n - 1/2^m)$, where f_b = 5 MHz is the incoming bunch rate and n is an integer. For n = 60, the cavities operate at 297.5, 298.75 and 299.375 MHz. The tree is also synchronous for odd subharmonics of 5 MHz.

The first two levels of the tree are designed to be achromatic and isochronous using the MAD code [10]. The kick from a pair of separator cavities is amplified by a horizontally focusing quadrupole which is on the input beam axis and therefore off axis for the deflected beams. The quadrupole is 90° in horizontal betatron phase downstream of the cavities. Further downstream, a DC double septum deflects the separated beams in opposite directions. The beams then propagate in separate vacuum chambers with the achromatic bends completed for each beam. A small reverse bend allows adjustment of R_{56}.

The first level requires a bend angle of 5°, so a second double-bend achromat was added for additional deflection. The net R_{56} of the combined arc is set to zero. The smaller deflections of the remaining two levels are obtained with single achromats. To reduce the effects of coherent synchrotron radiation, the horizontal beta functions are low within the large-angle bends.

The first level uses a unipolar split with no net deflection upstream of the 0.5 GeV linac in the 2.2 GeV path. This is accomplished by biasing the separator cavities with DC magnets to create a straight-through dispersion-free path with FODO optics. For a bunch that is sent to a 1.7 GeV FEL, Fig. 7 shows the first level.

In the similar second and third levels, a symmetrical angular deflection is used. After the last separation, a

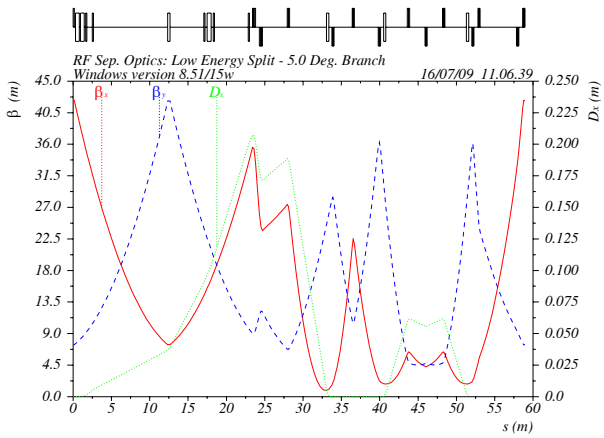

Figure 7: Lattice functions for the first level of the beam spreader, for a bunch that is sent to a 1.7 GeV FEL.

FODO-type transverse collimator and a dogleg energy collimator protect the FELs from off-axis and off-energy electrons. The combination of the third separation level and the collimators is designed to be achromatic and isochronous. Figure 8 shows the third level of the spreader and the transverse collimator. The dogleg energy collimator is shown in Fig. 9. Although the entire spreader (including the collimators) is designed with the MAD code [10] to have $R_{56} = 0$, the computed R_{56} value of our ELEGANT [7] model is 38.5 μm.

SUMMARY

The University of Wisconsin-Madison and MIT are developing a design for a multidisciplinary user facility with FELs operating in the VUV to soft x-ray range. The facility provides seeded, fully coherent output with tunable photon energy and polarization over the range 5–900 eV, and simultaneous independent operation of multiple FEL beamlines. The beamlines will support a wide range of science, including ultrashort pulses with kHz rates for femtochemistry, and high average flux with

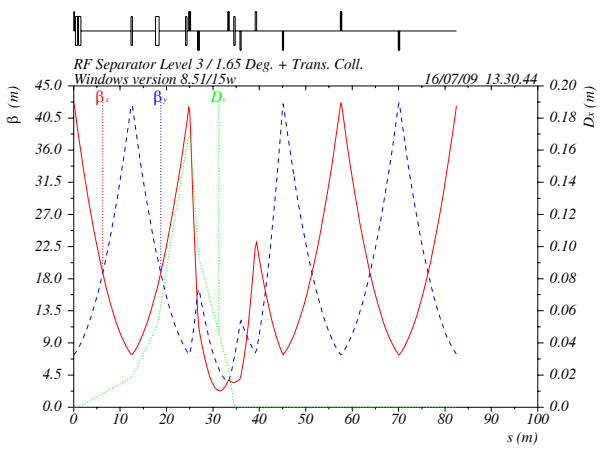

Figure 8: Lattice functions for the third spreader level and the transverse collimator.

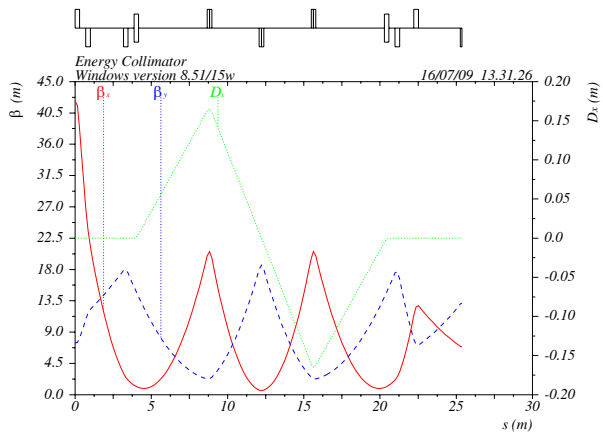

Figure 9: The dogleg energy collimator.

narrow bandwidth and MHz rates for photoemission spectroscopy. This unique facility is expected to enable new science through ultrahigh resolution in the time and frequency domains, as well as coherent imaging and nanofabrication.

REFERENCES

[1] J. Bisognano, R. Bosch, M. Green, H. Hoechst, K. Jacobs, K. Kleman, R. Legg, R. Reininger, R. Wehlitz, J. Chen, W. Graves, F. Kärtner, J. Kim and D. Moncton, in "Proceedings of the 2007 Particle Accelerator Conference, Albuquerque, NM" (IEEE, Piscataway, NJ, 2007), p. 1278.

[2] J. Bisognano, M. Bissen, R. Bosch, M. Green, K. Jacobs, H. Hoechst, K. Kleman, R. Legg, R. Reininger, R. Wehlitz, W. Graves, F. Kärtner and D. Moncton, in "Proceedings of the 2009 Particle Accelerator Conference, Vancouver, Canada" (IEEE, Piscataway, NJ, 2009), MO4PBC04.

[3] J. J. Bisognano, R. A. Bosch, M. A. Green, K. D. Jacobs, K. J. Kleman, R. A. Legg, J. Chen, W. S. Graves, F. X. Kärtner and J. Kim, in "Proceedings of the 2007 Particle Accelerator Conference, Albuquerque, NM" (IEEE, Piscataway, NJ, 2007), p. 1281.

[4] W. M. Fawley, Lawrence Berkeley Laboratory Report No. LBNL-49625 (2002).

[5] S. Reiche, Nucl. Instrum. Meth. A 429, 243 (1999).

[6] R. A. Bosch, K. J. Kleman and J. Wu, Phys. Rev. ST Accel. Beams 11, 090702 (2008).

[7] M. Borland, Advanced Photon Source Light Source Note LS-287, 2000.

[8] R. A. Bosch, K. J. Kleman and J. Wu, these proceedings.

[9] C. Leemann and C. G. Yao, in "Proceedings of the 1990 Linear Accelerator Conference LINAC'90, Albuquerque, NM" (Los Alamos Report No. LA-12004-C, 1991), p. 232.

[10] H. Grote, E. Keil, T. O. Raubenheimer and M. Woodley, in "Proceedings of the 7th European Particle Accelerator Conference, Vienna" (EPS, Geneva, 2000), p. 1390.